Application of eclipse laser photodetachment technique to electron sheath thickness and collection region measurements

Shin Kajita,[1,*] Shinichiro Kado,[2,†] Atsushi Okamoto,[2] and Satoru Tanaka[1]
[1]*Graduate School of Engineering, The University of Tokyo, Tokyo 113-8656, Japan*
[2]*High Temperature Plasma Center, The University of Tokyo, Tokyo 113-8656, Japan*
(Received 22 June 2004; published 15 December 2004)

The laser photodetachment (LPD) technique, which has been used for negative-ion density measurements, is applied for the measurement of electron sheath thickness and the collection region of photodetached electrons (PDE's). By forming a thin laser shadow in the laser beam channel, the electron sheath can be observed in the temporal evolution of the LPD signals. The collection region of PDE's is determined from the response of the signal peak value in scanning the shadow position. The measurement is applied to the electron sheath formed around a cylindrical probe and a plane probe. The experimentally obtained thickness of the sheath in front of the plane probe agrees well with the one-dimensional Child-Langmuir sheath when the magnetic field exists. Further, the results of the sheath thickness around the plane and cylindrical probe at different magnetic field strengths indicate that the effect of magnetic field on the sheath structure is significant even in weakly magnetized plasmas. The length of the collection region of PDE's was measured, and it was confirmed that the region was in the laser beam channel under our experimental conditions. It is proposed that this method be applied to check the validity of the laser photodetachment technique.

DOI: 10.1103/PhysRevE.70.066403 PACS number(s): 52.40.Kh, 32.80.Gc

I. INTRODUCTION

The laser photodetachment (LPD) technique assisted by means of an electrostatic probe has been widely used for negative-ion density and the drift velocity measurements [1]. In this measurement, the excess electrons, produced by the laser-induced photodetachment process $H^- + h\nu \rightarrow H + e^-$, are detected by an electrostatic probe. The negative-ion density is then deduced from the electron current (and therefore the density) response, which is called LPD signal. Temporal evolution of the LPD signal after the laser injection is strongly connected to the motions of both the negative and positive ions.

The temporal evolution of the excess electron density after the laser injection is well described by the hybrid fluid-kinetic model [2,3], in which negative ions are treated based on a ballistic kinetic theory [4], while the positive ions and electrons are treated based on fluid theory. The first half of the temporal evolution is mainly determined by the motion of negative ions, while the positive-ion effect is mainly appeared in the latter half of the LPD signal as a negative overshoot of the signal. Thus, the recovery time t_{recov}, defined as the period for the electron density in the center of the laser beam to recover to the initial density, has been interpreted as the time for the background negative ions to flow into the laser channel at the drift velocity [5,6].

However, the electron sheath and/or collection region around the electrostatic probe modify both the signal peak value and the temporal evolution, when they expand to a considerable length [1,7]. The collection region of the photodetached electrons (PDE's) required in the LPD measurement has been evaluated from the dependence of the signal intensity on the laser radius in Ref. [8]. The LPD signal intensity saturates for a laser radius larger than the collection region of PDE's, while it cannot attain the saturation value for a laser radius smaller than the region. It was also reported in Ref. [8] that the radius of the collection region of PDE's was about twice the calculated electron sheath thickness. When the magnetic field exists, however, the electron sheath will stretch along the field. Consequently, the collection region can also expand along the field.

Recently attention has been paid to the role of negative ions in the divertor region of experimental fusion reactors. The negative ions are expected to contribute to the enhancement of recombination processes which are capable of reducing the heat flux to the divertor plate [9,10]. The laser photodetachment technique has been applied to some linear divertor simulators for the negative ion density measurement [11,12]. Up to now, however, the validity of the laser photodetachment technique under the existence of a magnetic field has not been examined, so that it is necessary to understand the structure of the sheath and the collection region of PDE's around the electrostatic probe for the purpose of verifying the measurement. In this situation, it may be necessary to measure the sheath and collection region *in situ*.

Reliable measurement with high sensitivity and sufficient spatial resolution for the electric field or potential is necessary to understand the sheath structure around an electrostatic probe. Recently, a high-sensitivity measurement for the sheath electric field that makes use of the Stark effect, called fluorescence-dip spectroscopy, has been developed [13,14]. This measurement, which has mainly been applied to the ion sheath in front of a wafer for plasma processing, can also be applied to the electron sheath around the probe. However, it requires a rather complicated experimental system including two tunable lasers and a detection system with high efficiency.

*Electronic address: shin@flanker.q.t.u-tokyo.ac.jp
†Electronic address: kado@g.t.u-tokyo.ac.jp

We have developed a simple measurement method for the electron sheath thickness using modification of the temporal evolution of the Eclipse-LPD signal [15] alone. The Eclipse-LPD was originally developed for avoiding the probe surface ablation due to laser irradiation, which is unavoidable in high-electron-density plasmas [16]. In this method, a thin wire is inserted in a laser channel in order to form a shadow in the laser beam channel. We named this the "eclipse laser photodetachment method" after a lunar eclipse, in which the shadow of the Earth protects the Moon from irradiation by the Sun. It has been confirmed that the negative-ion signal is obtained without being disturbed by the shadow when the shadow width is sufficiently thinner than the laser size [15]. The effects of the sheath are observed in the temporal evolution of LPD or Eclipse-LPD signals, while those of the collection region of PDE's are observed in the behavior of the Eclipse-LPD signal intensity as the change of the relative displacement between the probe tip and shadow changes. Regarding *in situ* measurements of the collection region, use of the Eclipse-LPD is easier than the method in Ref. [8], in which the laser diameter is changed, to detect the required minimum diameter, i.e., the collection region of PDE's. This is because the shadow position can be changed continuously and be controlled remotely in the Eclipse-LPD.

The principle of the measurements is shown in Sec. II, and the experimental setup is briefly described in Sec. III. In Sec. IV, the measurements of the electron sheath and the collection region of PDE's are presented. Finally, the paper is concluded in Sec. V.

II. PRINCIPLES

A. Theoretical Child-Langmuir sheath

The sheath thicknesses can be estimated using the Child-Langmuir law assuming that the particle energy is sufficiently small compared to the potential of the sheath: namely, $T_e \ll e(V_p - V_{sp})$, where T_e is the electron temperature in eV, e the elementary charge, V_p the probe voltage, and V_{sp} the space potential. The electron sheath thickness in one-dimensional geometry can be written as [17]

$$h_p = \frac{2}{3}\sqrt{-\frac{\epsilon_0}{j}}\left(\frac{2e(V_p - V_{sp})^3}{m_e}\right)^{1/4}, \tag{1}$$

where j is the current density, ϵ_0 the dielectric constant in vacuum, and m_e the mass of an electron. In the present paper, h_p stands for the thickness of the "plane-parallel Child-Langmuir (CL) sheath" hereafter. This can be regarded as the limit of using a plane probe in magnetized plasmas.

On the other hand, in cylindrical geometry, the sheath thickness is expressed as a function of $\beta = (r_p + h)/r_p$, where r_p is the probe radius, and then can be written as [18]

$$h_c = -\frac{8\pi\epsilon_0}{9j\beta^2}\sqrt{\frac{2e}{m_e}}(V_p - V_{sp})^{3/2}. \tag{2}$$

h_c stands for the thickness of the "cylindrical CL sheath" in this paper. This can be regarded as the limit of using a cylindrical probe in unmagnetized plasmas. In the above expressions, it is assumed that the potential at the sheath edge is the space potential and that the velocity at the sheath edge is negligible. Because the electron velocity in the sheath is much faster than the thermal velocity as long as $T_e \ll e(V_p - V_{sp})$, this assumption applies in a comparison of the theoretical model and the experiment. In real situations, however, the potential at the sheath edge is different from the space potential, so that the electric field expands to the outside of the sheath edge to some extent [19].

B. Theoretical electron collection region

In the sheath region, the sharp potential gradient causes charge separation. In the presheath region, on the other hand, the potential varies slowly and quasineutrality is satisfied. The effect of the presheath is not critical for the estimation of the sheath thickness because the potential rise in the region is small. Assuming that all electrons at the sheath edge flow into the probe once they enter the sheath, the electron density at the sheath edge, n_{es}, is half the ambient electron density [20]: namely,

$$n_{es} = \frac{1}{2}n_e. \tag{3}$$

From the quasineutrality at the sheath edge, we obtain

$$n_{es} = n_i \exp\left(-\frac{e(V_{se} - V_{sp})}{kT_i}\right), \tag{4}$$

where n_i is the ion density at a sufficiently distant point from the probe surface and T_i the ion temperature. Then, analogous to the ion sheath formation, the potential at the sheath edge is obtained as a function of the ion temperature, as [19]

$$\frac{e(V_{se} - V_{sp})}{kT_i} = \ln(2). \tag{5}$$

When $T_i \ll T_e$, the effect of the electric field on the particle motion in the presheath is negligible, so that the electron flux to the sheath edge is mainly determined by diffusion. Because the electron sheath edge behaves as a virtual probe surface, modification of the sheath thickness changes the temporal evolution of the LPD signal as described in Sec. II C.

The LPD signal intensity is reduced unless sufficient excess electrons are supplied to the sheath edge. Thus, the collection region of PDE's, which stretches far outside the sheath edge, should be introduced. The LPD signal intensity is sensitive to the excess electron in this region, while the excess electron outside the region does not contribute to the peak value of the LPD signal.

Because radial diffusion of the particle is restricted in the magnetic field, it is most likely that the collection region of PDE's is elongated along the magnetic field. It should be noted that the length of the collection region of PDE's, L_{PDE}, is not necessarily equal to the length of the collection region of the bulk electron, L_{col}, which is the disturbance length for the surrounding plasmas in steady state, although both can be affected by the magnetic field. In strongly magnetized plas-

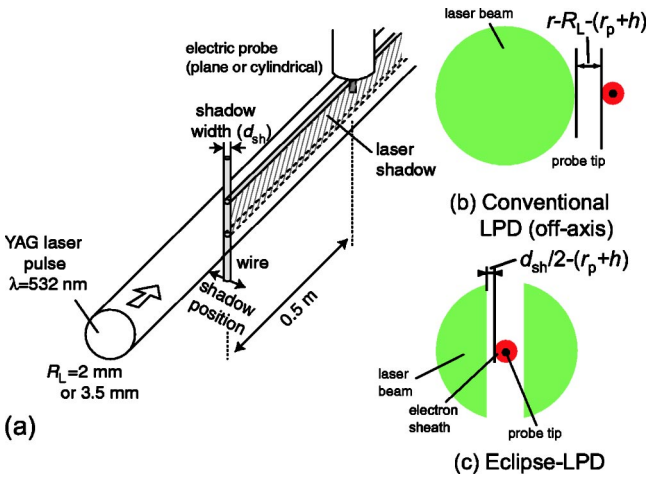

FIG. 1. (Color online) (a) Schematic view of experimental setup for the Eclipse-LPD method. (b) Configuration for off-axis conventional LPD for the sheath thickness measurements, where r is the distance from the center of the laser beam to the center of the probe tip. (c) Configuration for the Eclipse-LPD.

mas, where the electron Larmor radius is much smaller than the probe size, L_{col} can be roughly estimated by balancing the parallel particle flux to the probe with the cross-field particle flux to the collection region. For a collisionless case, the collection length is described as [21]

$$L_{col} \simeq \frac{v_{th}^{e} d^2}{D_{\perp}}, \tag{6}$$

where v_{th}^{e} is the thermal velocity of the electron, d the characteristic size of the probe, and $D_{\perp}$ the cross-field diffusion coefficient. The characteristic cross-field velocity is $v_{\perp} \simeq D_{\perp}/d$, and consequently,

$$L_{col} \simeq \frac{v_{th}^{e} d}{v_{\perp}}. \tag{7}$$

Since the cross-field velocity is much smaller than the parallel velocity in the strongly magnetized cases, L_{col} is expected to be much longer than the probe size. Moreover, in the usual case, the laser radius is several mm while the probe size is from several tenths of mm to several mm, and it can therefore be expected that L_{col} is longer than the laser beam radius in strongly magnetized plasmas. In contrast, the length of the collection region of photodetached electrons, L_{PDE} represents the region in which sufficient excess electrons are supplied without escaping until they arrive at the sheath. We focus on L_{PDE} in the present paper and a discussion of L_{col} is not within the scope of this paper.

C. Measurement of sheath thickness

A schematic view of the experimental arrangement of the Eclipse-LPD is depicted in Fig. 1(a). The configuration of the laser beam and probe tip in Eclipse-LPD and conventional off-axis LPD are shown in Figs. 1(b) and 1(c), respectively. The typical temporal evolution of the conventional on-axis LPD signal and that of Eclipse-LPD are shown in

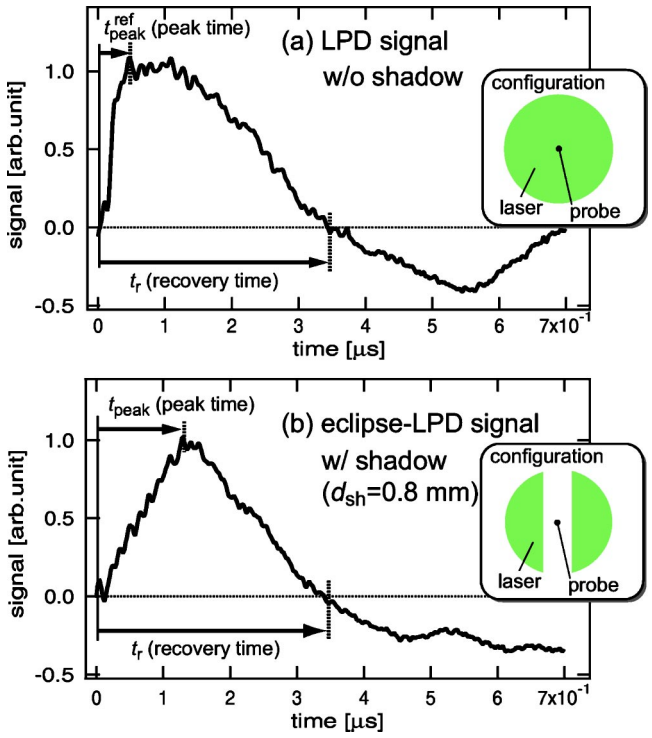

FIG. 2. (Color online) (a) Typical laser photodetachment signal for the probe located in the center of the laser diameter. (b) Typical eclipse laser photodetachment signal ($V_p - V_{sp}$=30 V).

Figs. 2(a) and 2(b), respectively. The recovery time t_{recov}, in which the electron density at the center of the laser beam recovers to the initial density, is expressed using the drift velocity of negative ions v_d and the radius of the laser beam, R_L [4].

Let us consider first the conventional on-axis LPD system. The recovery time of the LPD signal is expressed as

$$t_{recov} \simeq \frac{R_L - (r_p + h)}{v_d}, \tag{8}$$

where r_p represents the radius of the cylindrical probe tip and the half-thickness of the plane probe tip. h is the thickness of the electron sheath. Because the sheath thickness is negligible at the space potential, the recovery time at the space potential t_{recov0} is deduced by substituting h=0 in Eq. (8), as follows:

$$t_{recov0} \simeq \frac{R_L - r_p}{v_d}. \tag{9}$$

Thus, the sheath thickness is obtained from Eqs. (8) and (9), as

$$h \simeq \frac{(t_{recov0} - t_{recov})(R_L - r_p)}{t_{recov0}}. \tag{10}$$

We have checked that the recovery time is not disturbed by the shadow of the eclipse when the shadow width is sufficiently thinner than the laser diameter. Thus the sheath effects can be observed as a shift of the recovery time in both Eclipse-LPD signals and conventional LPD signals.

On the other hand, the time for the LPD signal to reach its peak value depends on the displacement between the effective probe surface including the sheath and edge of the photodetached electron *swarm*. The minimum value of this peak time t_{peak}^{ref} is the case of using conventional on-axis LPD because the displacement is zero, as shown in Fig. 2(a). When the probe is located outside the laser-irradiated area as shown in Fig. 1(b), the peak time of the signal is shifted by Δt_{peak} from t_{peak}^{ref}. Because the propagation velocity of the excess electron *swarm* toward the outside of the laser beam corresponds to the negative-ion drift velocity, the time shift due to the propagation can be expressed from Fig. 1(b) as [4]

$$\Delta t_{peak}(r,h) = t_{peak}(r,h) - t_{peak}^{ref} \simeq \frac{r - R_L - (r_p + h)}{v_d} \quad (>0), \tag{11}$$

where r is the distance from the center of the laser beam and the term (r_p+h) represents the probe radius corrected by the sheath thickness.

In the same manner, when a thin laser shadow is formed in the laser beam, the excess electron *swarm*, which travels inward, reaches the probe surface with the time shift

$$\Delta t_{peak}(h) = t_{peak}(h) - t_{peak}^{ref} \simeq \frac{d_{sh}/2 - (r_p + h)}{v_d} \quad (>0), \tag{12}$$

where d_{sh} is the shadow width. This expression is similar to that in Eq. (11) except that the configuration of Fig. 1(c) is applied. The shift of the peak time at the space potential, Δt_{peak0}, can be also deduced by substituting $h=0$ in Eq. (12) as

$$\Delta t_{peak0} = t_{peak}(h=0) - t_{peak}^{ref} \simeq \frac{d_{sh}/2 - r_p}{v_d}. \tag{13}$$

Finally, the electron sheath thickness is deduced from the difference between Eqs. (12) and (13) as

$$h \simeq (\Delta t_{peak0} - \Delta t_{peak}) v_d, \tag{14}$$

where v_d can be obtained, Eq. (9).

A typical Eclipse-LPD signal is shown in Fig. 2(b), in which the peak time is shifted from that of the conventional LPD signal shown in Fig. 2(a). In the conventional LPD method, the peak time shift cannot appear unless the probe is situated outside the laser beam (off-axis geometry)—i.e., $r - R_L > r_p + h$. However, in the off-axis geometry, the signal intensity apparently decreases as r increases, when $r > R_L$. In the Eclipse-LPD method, on the other hand, the sheath effect can be observed in the on-axis geometry without the reduction of the signal intensity [15]. From Eqs. (8) and (12), the sheath thickness is obtained as

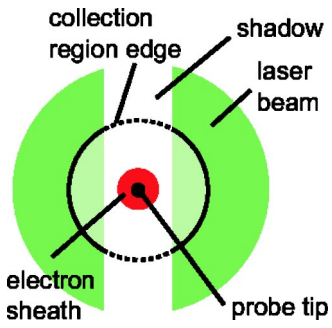

FIG. 3. (Color online) Sheath thickness and collection region in the Eclipse-LPD geometry.

$$h \simeq \frac{(d_{sh}/2 - r_p)t_{recov} - (R_L - r_p)\Delta t_{peak}}{\Delta t_{peak} + t_{recov}}. \tag{15}$$

Therefore, in the Eclipse-LPD method, we can obtain the sheath thickness h in three independent ways. However, use either of Eq. (10) or of Eqs. (14) and (9) requires two signals at different bias voltages, space potential, and positive bias. In contrast, there is a significant merit in the application of Eq. (15) because sheath thickness can be measured from a single signal at any bias voltage. Note that the width of the shadow, d_{sh}, is necessary in the case of using Eq. (15). The shadow width at the probe tip is somewhat thicker than the diameter of the inserted wire due to the diffraction of the laser beam. The diffraction effect on the results will be discussed later in Sec. IV A.

D. Measurement of collection region

As mentioned above, the time evolution of the LPD signal depends mainly on the electron sheath thickness. On the other hand, the intensity of the LPD signal is sensitive to the collection region of PDE's that is stretched to the outside of the electron sheath edge. In the Eclipse-LPD method shown in Fig. 3, the signal intensity decreases when part of the collection region is covered by the shadow. However, the signal intensity recovers when the shadow is well aligned with the electrostatic probe. This phenomenon can be explained by the excess electrons leaked to the nonirradiated shadow region from the irradiated region. The width of the total signal dip is $2(L_{PDE}+r_p+d_{sh}/2)$. We can thus obtain L_{PDE} from the width of the signal dip.

III. EXPERIMENTS

The experiments were performed in the downstream chamber of a linear divertor simulator MAP-II [11,22]. The plasma was generated using helium discharge, and additional hydrogen gas was injected into the downstream chamber. The central electron density n_e and the temperature T_e were about 1×10^{12} cm^{-3} and 5 eV, respectively, while those at the peripheral region were about 1×10^{11} cm^{-3} and 1.5 eV, respectively. The electrostatic probe was located at the peripheral region of the plasma column, where the ratio of the negative-ion density to the electron density is about several

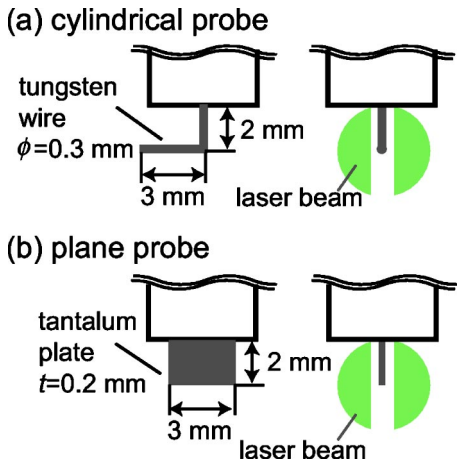

FIG. 4. (Color online) Two types of probes used for the experiments. (a) An L-shaped cylindrical probe. (b) A plane probe.

percent [11,23]. We neglected the modification of the sheath structure due to the photodetachment process, because the negative-ion density was much smaller than the electron density. For the purpose of investigating the dependence of the probe shape on the sheath structure, we used two types of probe as shown in Fig. 4. One was an L-shaped cylindrical probe, which was made of a 0.3-mm tungsten wire. The length exposed to the plasma was totally 5 mm. The other was a plane probe made of a tantalum plate 0.2 mm in thickness and 3 mm$\times$2 mm dimensions. A magnetic field of 15 mT was applied, and the effect of the field was examined by comparing to the case without the magnetic field. In reality, a weak magnetic field of less than 1 mT exists even when the coil currents at the downstream chamber are turned off. However, the effect is negligible because the Larmor radius of electrons is much larger than the probe size in this case. Thus, we henceforth call this condition 0 mT. In the case of 15 mT, the Larmor radius of the electrons is comparable to the diameter of the cylindrical probe but much smaller than the plane probe size. Thus, we can expect that the sheath structures for a plane probe at 15 mT and for a cylindrical probe at 0 mT correspond to the plane-parallel (h_p) and cylindrical (h_c) CL sheaths, respectively. Second-harmonic Nd:YAG laser pulses (wavelength of λ=532 nm) were used for the photon source of the photodetachment. For the Eclipse-LPD, a thin wire, which is located outside the vacuum chamber, was installed in the laser beam path. The distance from the wire to the probe tip was about 0.5 m and the shadow position was adjusted by a micrometer of the wire stage.

IV. RESULTS AND DISCUSSION

A. Electron sheath

In order to examine the sheath effect on the temporal evolution of the LPD signal, the recovery time t_{recov} and the peak time t_{peak} of LPD signal are plotted against probe voltage in Fig. 5. Figure 5(a) is the case of the plane probe at 15 mT, while Fig. 5(b) is the case of a cylindrical probe at 0 mT.

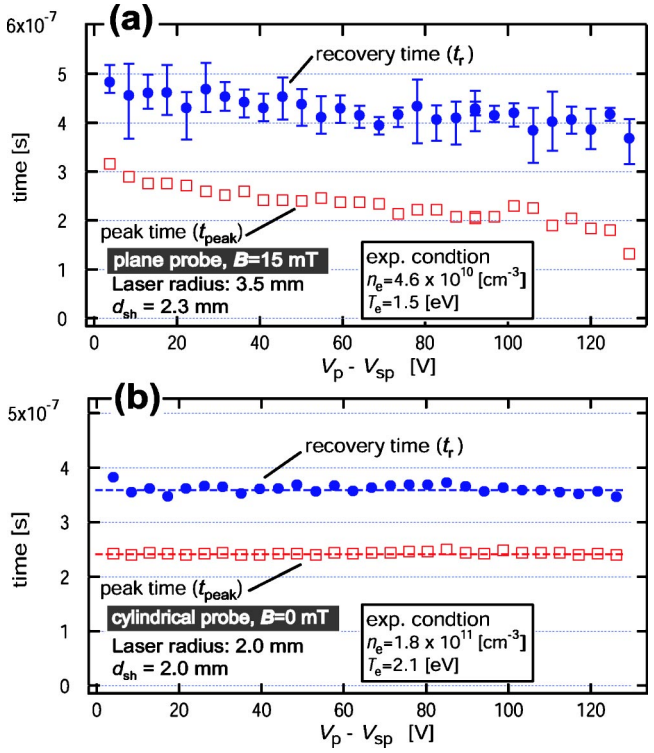

FIG. 5. (Color online) Recovery time and peak time as a function of probe-bias voltage. (a) A plane probe at 15 mT (b) A cylindrical probe at 0 mT (shot Nos. 15441, 14393).

Both t_{recov} and t_{peak} were significantly reduced as the probe voltage increased in Fig. 5(a), while time shift was not observed either on t_{recov} or t_{peak} in Fig. 5(b). These reductions in Fig. 5(a) are attributed to the expansion of sheath thickness with the probe voltage. The comparison between Figs. 5(a) and 5(b) shows that the thickness of sheath around the cylindrical probe at 0 mT is much thinner than that around the plane probe at 15 mT.

As mentioned in Sec. II, the sheath thickness can be deduced from the results in Fig. 5(a) in three ways. Figure 6(a) shows the electron sheath thicknesses obtained (i) from Eq. (10), (ii) from Eqs. (14) and (9), and (iii) from Eq. (15), respectively, together with the calculated h_p and h_c. The thickness in cases (i) and (ii) agree with each other and also agree with the plane-parallel CL sheath. This result is the one we expected.

In contrast, the sheath thickness in case (iii) in Fig. 6(a) is considerably lower than that in cases (i) and (ii). This is due to the diffraction of the laser beam resulting from the wire at a distance of 0.5 m from the probe location. Our calculation based on the Fresnel diffraction theory shows that the width of the region where laser power is reduced at the probe location is about 0.6 mm wider than the wire diameter. An effective shadow width at the probe location is revealed to be the wire diameter plus 0.6 mm in this case. The modified values of (iii) are plotted in Fig. 6(a) as in case (iii)′. The underestimation in case (iii) was sufficiently compensated. Note that the diffraction effect is canceled when Eq. (10) or Eqs. (14) and (9) are used. The result of case (iii)′ confirms the validity of the measurement of electron sheath thickness using Eq. (15).

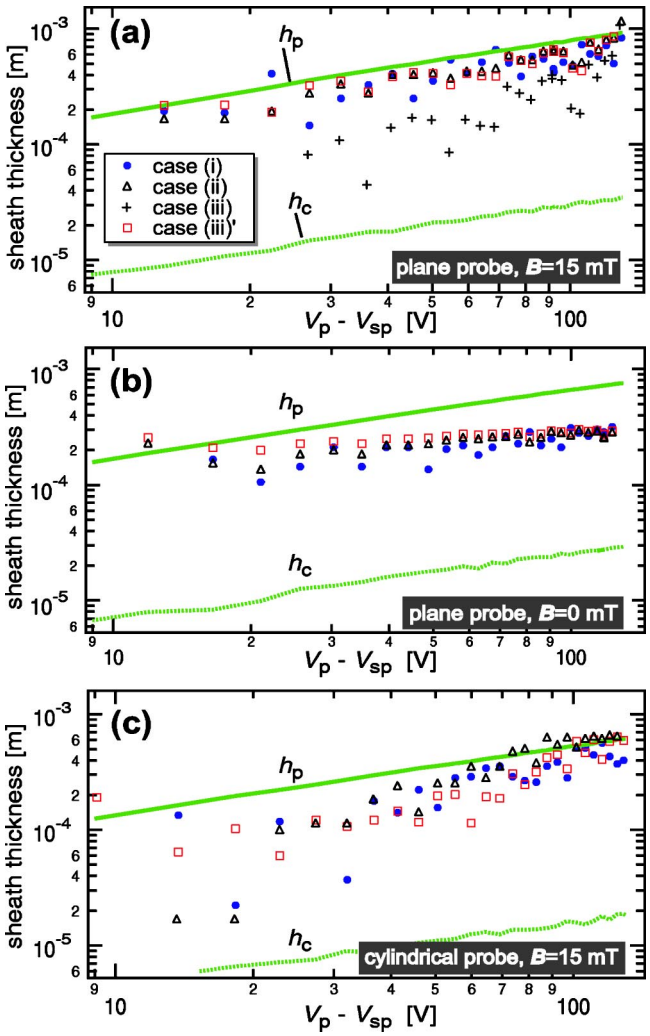

FIG. 6. (Color online) Comparisons of experimentally obtained electron sheath thicknesses, (i) from Eq. (10), (ii) from Eqs. (14) and (9), and (iii) from Eq. (15) using the wire diameter for the shadow width. (iii)′ is the modified values of (iii) by taking diffraction effect into consideration. Theoretical sheath thickness using Child-Langmuir law deduced from Eqs. (1) and (2) is shown as the solid (h_p) and dotted (h_c) lines, respectively. (a) is the case for a plane probe at 15 mT, (b) for a plane probe at 0 mT, and (c) for a cylindrical probe at 15 mT ($n_e=5\times10^{10}-1\times10^{11}$ cm^{-3} and $T_e=1.5$ eV) (shot Nos. 15441, 15402, 13926).

The sheath thicknesses were also measured under other conditions. Figures 6(b) and 6(c) show the probe voltage dependence of the sheath thickness at 0 mT using a plane probe and at 15 mT using a cylindrical probe, respectively. As shown in Fig. 5(b), the change of t_{recov} and t_{peak} is so small in the case of the cylindrical probe at 0 mT that it is difficult to deduce the sheath thickness. In fact, h_c is much thinner than 0.1 mm under our experimental condition as shown in Fig. 6. Both in Figs. 6(b) and in 6(c), the three calculation processes (i), (ii), and (iii)′ give values consistent with each other, as they do in Fig. 6(a).

It can be seen in Fig. 6(b) that the experimentally obtained sheath thickness is thinner than h_p by a factor of 2–3 but thicker than h_c. In this situation, the sheath thickness is about 0.2 mm when, for example, V_p-V_s is around 100 V. Taking the probe size into consideration, the dimension of the cross section of the sheath is about 0.6 mm times 3.4 mm, assuming that the sheath is formed around the probe tip uniformly, so that the front face of the probe surface is significantly larger than the side face of the probe surface. However, because the current flow is not completely one dimensional in this case, the geometrical relation between the probe tip and the sheath edge is more like a plane anode and a concave cathode than like plane-plane geometry. Therefore, the edge of the sheath is less affected by the bias in the high-voltage regime. We think that this is the main reason for the difference between the experiment and calculation at higher probe voltage shown in Fig. 6(b).

On the other hand, in Fig. 6(c), the sheath thickness is close to h_p at higher probe bias than 50 V, although the Larmor radius of the electron is comparable to the diameter of the probe tip. The results in Fig. 6(c) show that the electron sheath structure is affected by the existence of the magnetic field, even in a weakly magnetized regime for electrons.

It can be said from these results that the method in Sec. II C can be used for the measurement of electron sheath thickness around the electrostatic probe when the negative ion exists in the plasmas and the sheath has considerable thickness (typically $\gtrsim$0.1 mm). These results also indicate that the sheath thickness should be taken into account for the measurement of the drift velocity of negative ions from t_{recov} or Δt_{peak}, especially when the magnetic field exists. Although the contribution of negative ions to the sheath is neglected in this paper, the application of this method can be expanded to situations in which the ratio of the negative-ion density to the electron density is high, by minimizing the laser power so as not to alter the sheath structure in response to the photodetachment process.

B. Collection region

Figure 7 shows the Eclipse-LPD signal intensity as a function of the shadow position. A cylindrical probe biased to 60 V was used in this case, and the magnetic field strength was 15 mT. The signal intensity decreased when the collection region was covered by the shadow, so that the width of the total signal dip was $2(L_{PDE}+r_p+d_{sh}/2)$. The width of the signal groove obtained in the shadow position dependence of the intensity, shown in Fig. 7, gives the collection length. Moreover, the sheath thickness h is obtained from the temporal evolution of the Eclipse-LPD signal at *shadow position*=0 mm by using Eq. (15).

Figure 8 shows the experimentally obtained length of the collection region, L_{PDE} and h at different probe-bias voltages. The magnetic field strength was 15 mT, and the electron density and temperature were about 10^{11} cm^{-3} and 1.5 eV, respectively. The effective shadow width at the probe location, *wire diameter* plus 0.6 mm, was used to deduce h and L_{LPD}. Both h and L_{PDE} increase with probe-bias voltage. The length L_{LPD} was about 3–5 times thicker than h. Ten times the Debye length λ_D, where $\lambda_D=(\epsilon_0 T_e/n_e e^2)^{1/2}$, is also plotted in Fig. 8, based on the fact that $5\lambda_D-10\lambda_D$ is conven-

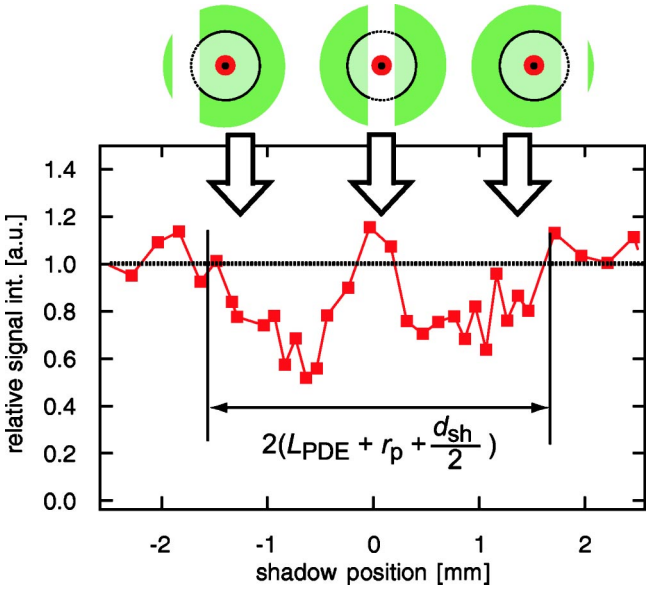

FIG. 7. (Color online) The shadow position dependence of the LPD signal intensity (shot No. 13692). Top figures represent the relative position of the shadow depicted in Fig. 3.

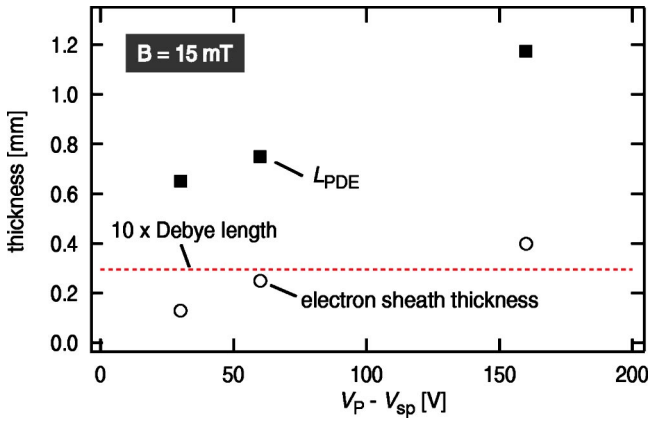

FIG. 8. (Color online) Experimentally obtained collection length of PDE L_{PDE} and electric sheath thickness at different probe-bias voltages. The dotted line represents 10 times the Debye length ($n_e = 1 \times 10^{11}$ cm^{-3}, $T_e = 1.6$ eV) (shot Nos. 14242, 13692, 14206).

tionally considered as the typical sheath thickness. Figure 8 shows that the sheath thickness is comparable to 10 times the Debye length when the probe is positively 70–80 V biased against space potential.

The dependence of the h_p on the electron density and the temperature is obtained by substituting

$$j = -\frac{1}{4} n_e e \sqrt{\frac{8kT_e}{\pi m_e}} \tag{16}$$

into Eq. (1), as follows:

$$h_p = \frac{2}{3}\sqrt{\frac{2\epsilon_0}{n_e}}\left(\frac{\pi(V_p - V_{sp})^3}{ekT_e}\right)^{1/4}. \tag{17}$$

h_p is a decreasing function of n_e and T_e. When n_e is rather low, typically less than 10^{10} cm^{-3}, h_p can be comparable to or longer than the laser radius, even in weakly magnetized plasmas, and, consequently, L_{PDE} is several times longer than h_p. Thus, it is strongly recommended that the sheath thickness and L_{PDE} be checked using the methods developed in this paper, when the laser photodetachment technique is applied to low-electron-density plasmas even though the magnetization is weak. Moreover, in strongly magnetized plasmas, it may be especially important to check whether the L_{PDE} is less than the the laser beam radius.

V. CONCLUSIONS

A measurement method of electron sheath thickness using the time evolution of the eclipse laser photodetachment signal has been developed. The electron sheath thickness around a plane probe and a cylindrical probe was measured in two kinds of magneticfields, about 15 mT and 0 mT. Three different derivation processes using the recovery time and peak time shift deduced values equal to each other and the validity of the methods was confirmed. The measurement using the Eclipse-LPD method is especially useful as the Eclipse-LPD method requires only a single probe bias if the diffraction of the laser is taken into account. This work has shown that the electron sheath thickness is very sensitive to the magnetic field. The sheath thickness almost obeys the plane-parallel CL sheath even in a weak magnetic field of 15 mT.

The electron collection region of photodetached electrons is also measured from the shadow position dependence of the LPD signal intensity. Under the experimental conditions of the present paper, the length of the electron collection region was 3–5 times longer than the electron sheath thickness. The laser photodetachment signal intensity is reduced when the collection region is longer than the laser radius, and the recovery time is reduced when the electron sheath thickness is considerably thick. The methods developed in this paper are shown to be capable of checking the applicability of the laser photodetachment technique by using the technique itself.

ACKNOWLEDGMENTS

The authors would like to thank Professor B. Xiao for useful discussions. One of the authors (S. Kajita) was partly supported through the 21st Century COE Program, "Mechanical Systems Innovation," by the Ministry of Education, Culture, Sports, Science and Technology of Japan.

[1] M. Bacal, Rev. Sci. Instrum. **71**, 3981 (2000).
[2] L. Friedland, C. I. Ciubotariu, and M. Bacal, Phys. Rev. E **49**, 4353 (1994).
[3] M. Nishiura, M. Sasao, M. Wada, and M. Bacal, Phys. Rev. E **63**, 036408 (2001).
[4] R. A. Stern, P. Devynck, M. Bacal, P. Berlemont, and F. Hillion, Phys. Rev. A **41**, 3307 (1990).
[5] M. Nishiura, M. Sasao, and M. Bacal, J. Appl. Phys. **83**, 2944 (1998).
[6] M. Nishiura, M. Sasao, Y. Matsumoto, M. Hamabe, M. Wada, H. Yamaoka, and M. Bacal, Rev. Sci. Instrum. **73**, 973 (2002).
[7] M. Bacal, Plasma Sources Sci. Technol. **2**, 190 (1993).
[8] M. Bacal, A. M. Bruneteau, and M. Nachman, J. Phys. (Paris) Lett. **42**, L-5 (1981).
[9] R. K. Janev, D. E. Post, W. D. Langer, K. Evans, D. B. Heifetz, and J. C. Weisheit, J. Nucl. Mater. **121**, 10 (1984).
[10] I. Krasheninnikov, A. Yu. Pigarov, and D. J. Sigmar, Phys. Lett. A **214**, 295 (1996).
[11] S. Kajita, S. Kado, N. Uchida, T. Shikama, and S. Tanaka, J. Nucl. Mater. **313–316**, 748 (2003).
[12] A. Tonegawa, M. Ono, Y. Morihira, H. Ogawa, T. Shibuya, K. Kawamura, and K. Takayama, J. Nucl. Mater. **313–316**, 1046 (2003).
[13] U. Czarnetzki, D. Luggenholscher, and H. F. Dobele, Phys. Rev. Lett. **81**, 4592 (1998).
[14] K. Takizawa, K. Sasaki, and A. Kono, Appl. Phys. Lett. **84**, 185 (2004).
[15] S. Kajita, S. Kado, A. Okamoto, T. Shikama, B. Xiao, Y. Iida D. Yamasaki, and S. Tanaka in *Proceedings of the 31st EPS Conference on Plasma Physics*, London, 2004, No. P 2.123 (unpublished).
[16] S. Kajita, S. Kado, T. Shikama, B. Xiao, and S. Tanaka, Contrib. Plasma Phys. **44**, 607 (2004).
[17] Y. P. Raizer, *Gas Discharge Physics* (Springer-Verlag, Berlin, 1991).
[18] I. Langmuir and K. B. Blodgett, Phys. Rev. **22**, 347 (1925).
[19] R. E. Kiel, AIAA J. **6**, 708 (1968).
[20] F. F. Chen, *Electric Probes, Plasma Diagnostic Technique* (Academic, New York, 1965).
[21] P. C. Stangeby, in *Plasma Diagnostics Vol. 2 Surface Analysis and Interactions*, edited by O. Auciello and D. L. Flamm (Academic, San Diego, 1989).
[22] S. Kado, H. Kobayashi, T. Oishi, and S. Tanaka, J. Nucl. Mater. **313–316**, 754 (2003).
[23] S. Kado, S. Kajita, D. Yamasaki, Y. Iida, B. Xiao, T. Shikama, T. Oishi, A. Okamoto, and S. Tanaka, J. Nucl. Mater. (to be published).